CWE-8
June 7-11, 2026
London, ON, Canada

Large-Eddy Simulation of key phases of racing wheelchair athlete motion

W Dixon [a], V Goosey-Tolfrey [b], G Page [a], D Butcher[a]

[a]*Department of Aeronautical and Automotive Engineering, Loughborough University, Loughborough, Leicestershire, United Kingdom, w.r.dixon@lboro.ac.uk*
[b]*School of Sport, Exercise and Health Sciences, Loughborough, Leicestershire, United Kingdom*

SUMMARY

This work utilised Large-Eddy Simulation (LES) to gain an understanding of how the drag area of a racing wheelchair varies with athlete position. Three key positions of the stroke cycle were selected: catch, release and recovery. The analysis of the drag force revealed that the wheelchair contributes to over half the drag throughout the stroke cycle. However, the changes in the drag force across the stroke cycle are driven by the athlete's position, particularly the arms and torso. The time-averaged flow fields reveal the large changes in wake structures that occur across the stroke cycle as the athlete's position changes. This provides a baseline which can be used to inform potential methods to reduce the drag of a racing wheelchair athlete, such as positional or equipment changes.

Keywords: *Racing Wheelchair, Sports Aerodynamics, Para Sport, CFD*

1. INTRODUCTION

Wheelchair racing is a sport where results are often separated by tenths of a second; hence, minimising resistive forces is crucial for performance. At the typical racing speeds, aerodynamic drag accounts for at least 70% of the total resistive force (Forte et al., 2018). The propulsion of a racing wheelchair involves a highly dynamic movement which includes significant changes to the athlete's body position, presenting a complex aerodynamic problem. The stroke of a wheelchair racer can be broken down into two distinct phases, the propulsive phase and the recovery phase (Vanlandewijck et al., 2001). Three key static positions can be extracted from these phases: the start of the propulsive phase (catch), the end of the propulsive phase (release) and the midpoint of the recovery phase. Considering these three positions, Computational Fluid Dynamics (CFD) and experimental (wind tunnel) testing will be used in this work to help understand the major contributors to drag and inform on methods to reduce aerodynamic drag and maximise results.

2. COMPUTATIONAL METHODOLOGY

A generic model was generated by combining known athlete measurements from the literature with the DINED Anthropometric database, created by TU Delft (Molenbroek, 2018). The generic model was manipulated into the three positions using a virtual skeleton methodology (Giljarhus et al, 2023). The project partner, RGK Wheelchairs, supplied the racing wheelchair geometry.

The computational domain was designed to closely replicate the wind tunnel dimensions used for the experimental part of this research, which was performed at one-third scale. The domain has a length of 10.83m, a constant height of 1.32m, and a width that expands from 1.92m at the inlet to 1.94m at the outlet, reducing the adverse pressure gradient that would otherwise be present due to boundary layer growth. The geometry was prepared for meshing using the surface wrapper tool to ensure a watertight surface mesh, thereby avoiding issues when generating the volume mesh.

0.5mm cells were used on the surface; the boundary layer was resolved using 20 prism layers, with a first cell height of 0.005mm and a total height of 2.4mm, resulting in a y+ value of less than one. The growth rate from the surface mesh to the volume mesh was set at 1.2 to allow a smooth transition from the boundaries to the core polyhedral mesh. Additional volumetric refinements were included around the athlete and wheelchair and extend 1.2m behind the athlete. The final mesh consisted of around 90 million cells with some variation for each of the positions. A representative slice of the final mesh can be seen in Figure 2.

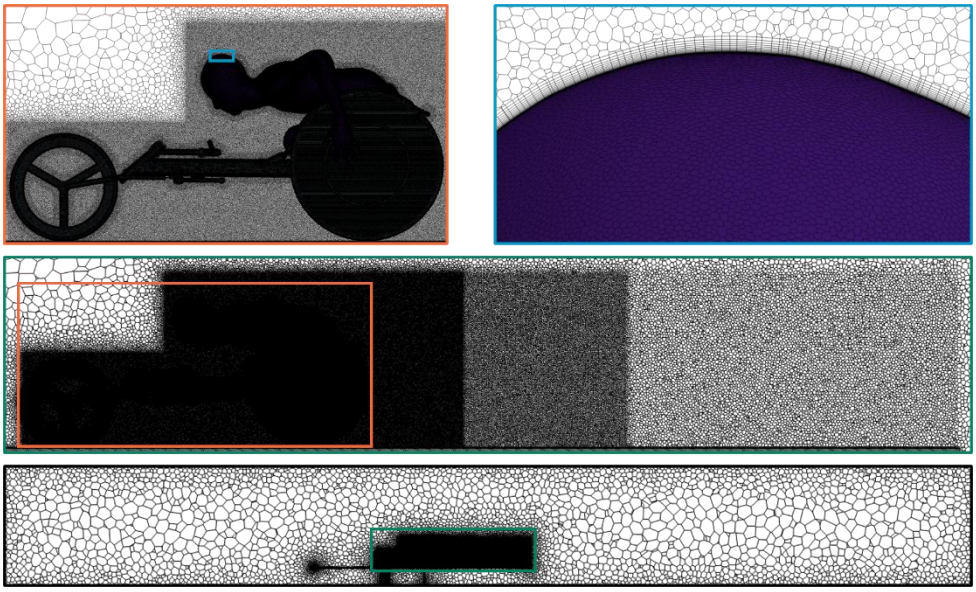

Figure 1 – Representative volume mesh slice along XZ plane showing:
[Top Left] Local refinement around the wheelchair and the athlete,
[Top Right] Surface mesh and prism layers,
[Middle] Volumetric wake refinement region,
[Bottom] Full computational domain

The inlet velocity of 24 m/s was selected to ensure Reynolds number similarity with the appropriate full-scale case. A no-slip wall condition was applied to the athlete and wheelchair, with no surface roughness applied. Simulations were conducted using StarCCM+ (Siemens, 2023), employing an LES approach with the Wall-Adapting Local Eddy-Viscosity (WALE) model to capture the flow unsteadiness. The timestep was set to 1E-5 seconds, which satisfied the Courant-Friedrichs-Lewy (CFL) condition. The mesh resolved more than 80% of the turbulent kinetic energy, thereby reducing numerical dissipation. The simulations were run for 4 seconds, with the final 3 seconds used for time-averaged analysis to ensure statistical convergence of the flow field.

3. RESULTS

3.1. Drag Force

The measured drag areas ($C_D A$) from each of the positions can be seen in Table 1. The catch position had the highest drag, followed by the release and then the recovery position. Each of these drag areas was within 3% of the experimental value, showing good correlation between the two measurements.

Table 1 – Reported drag area values for each position

Position	Drag Area (m^2)
Catch	0.0248
Release	0.0227
Recovery	0.0184

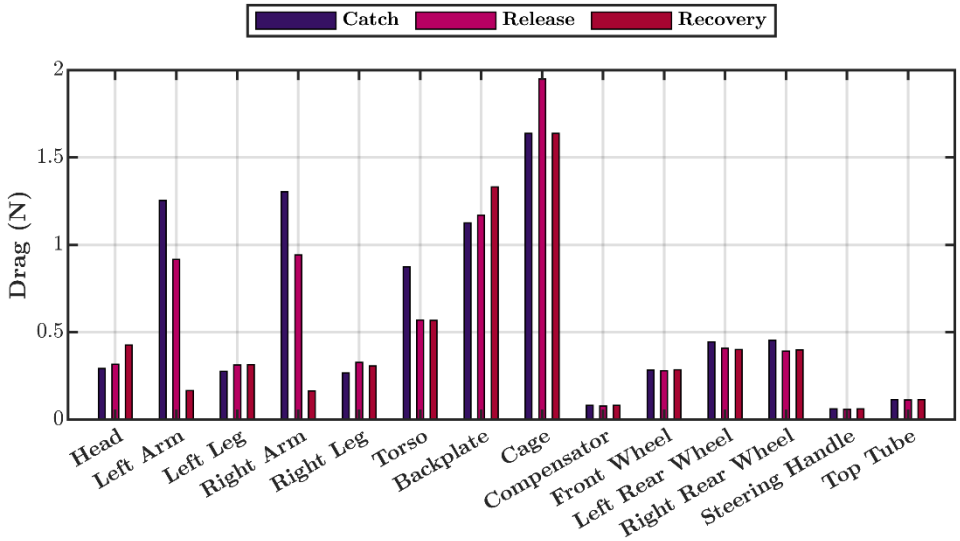

Figure 2 – Breakdown of drag force for each component

A detailed breakdown of each body part and chair component to the overall drag force can be seen in Figure 3. This indicates that the wheelchair is the primary source of drag; however, the athlete's position is the major influence on the drag force. The interaction between the athlete and the wheelchair means that as the athlete's position changes, this not only changes the percentage contribution, but also the absolute drag acting on it. The drag acting on the wheelchair decreases marginally as the athlete moves through the push cycle from catch to recovery, with the main changes coming from the contributions from the cage and backplate. Meanwhile, for the athlete, from catch to release, there is a 25% reduction in drag and a further 50% drop from release to recovery. The drop from catch to release is due to the combined effects of the movement of the arms and the torso, which reduces the frontal area. The further reduction from release to recovery primarily results from the arms being brought back close to the body, resulting in a more streamlined position.

3.2. Flow field analysis

Time-averaged flow field data are shown in Figure 3, illustrating the large changes in wake topology that occur at different points throughout the stroke cycle. In all positions, regions of velocity deficit form around the athlete's head and behind the wheelchair. In the catch position, the athlete's frontal area is at a maximum due to the elevated torso and arm position. This leads to a prominent recirculation region forming as the flow leaves the athlete's torso, which prevents the downward tapered wake structure visible in the release and recovery positions. The YZ plane slices further reveal the distinct structures contained within the flow: the catch phase exhibits strong asymmetrical vortical structures, whereas the release and recovery phases display more symmetric flows. In particular, the release phase features paired vortices shed from the arms, while the

recovery phase shows a vortex pair generated as the flow leaves the outstretched arms. These variations in the flow structure throughout the stroke cycle highlight the sensitivity of the overall flow to the athlete's position. The full paper will extend this work by providing a more detailed analysis of the unsteady LES.

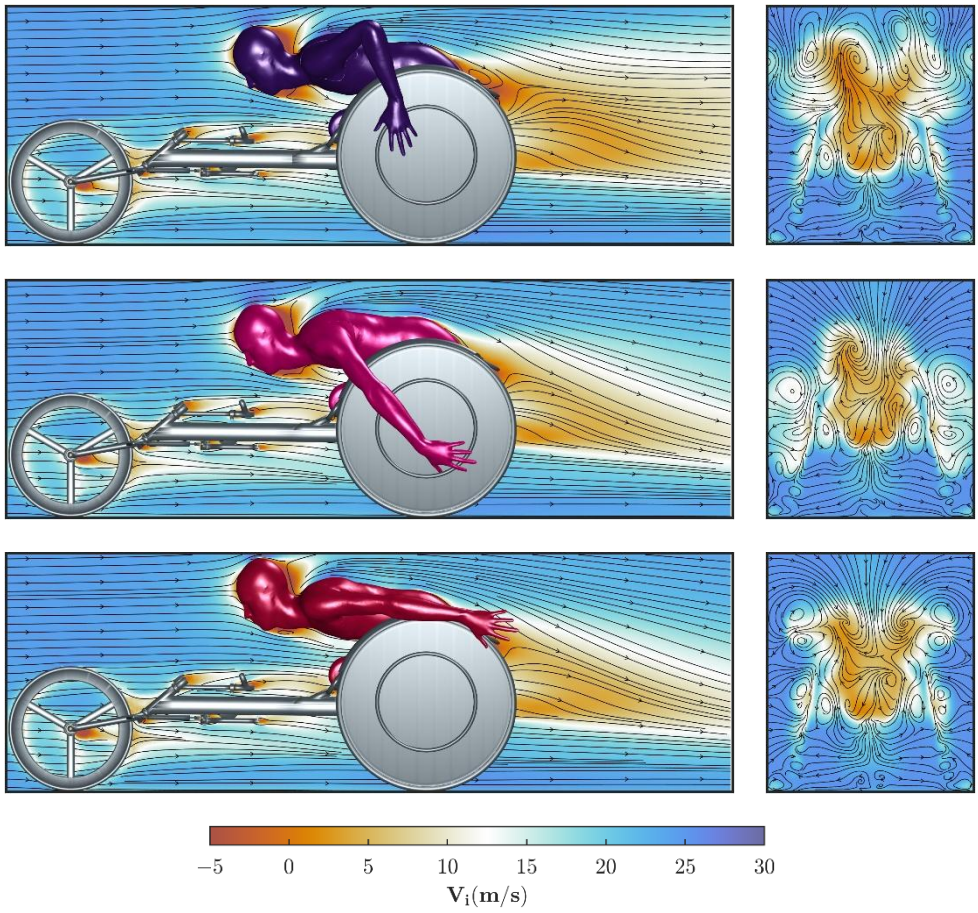

Figure 3 – Time Averaged Streamwise Velocity for each position
[Top] Catch, [Middle] Release, [Bottom] Recovery,
[Left] XZ (Y=0.00 m), [Right] YZ (X=0.35 m)

ACKNOWLEDGEMENTS

The author acknowledges the support of the Peter Harrison Foundation and RGK wheelchairs for their financial support and provision of a wheelchair model.

REFERENCES

Forte P, Barbosa TM, & Marinho DA. Technologic Appliance and Performance Concerns in Wheelchair Racing–Helping Paralympic Athletes to Excel New Perspectives in Fluid Dynamics, Chaoqun Liu (Ed.), InTech; 2015; 101–121

Vanlandewijck Y, Theisen D, Daly D. Wheelchair propulsion biomechanics: implications for wheelchair sports. Sports Med. 2001;31(5):339-67. doi: 10.2165/00007256-200131050-00005. PMID: 11347685.

Molenbroek, J.F.M. (Johan) (2018): DINED - anthropometric database. Version 1. 4TU.ResearchData. collection. https://doi.org/10.4121/uuid:199467d8-5c40-4a1f-a2f2-f2040db26270

K. E. T. Giljarhus, F. F. Liland, and L. Oggiano, “Virtual skeleton methodology for athlete posture modification in CFD simulations,” *Sports Engineering*, vol. 26, no. 1, Aug. 2023, doi: https://doi.org/10.1007/s12283-023-00430-8.